

## An efficient OFDM-based system with an insufficient cyclic prefix via a novel constellation algorithm

Saeed GHAZI-MAGHREBI\*

Department of Communications, College of Electrical Engineering, Yadegar-e- Imam Khomeini (RAH) Shahre Rey Branch, Islamic Azad University, Tehran, Iran

Received: 06.06.2015

Accepted/Published Online: 01.09.2016

Final Version: 29.05.2017

**Abstract:** In this paper, a new special triangular constellation scheme is introduced to replace the commonly used rectangular QAM constellation in orthogonal frequency division multiplexing (OFDM) modulation. We have shown that this new scheme has 3 major advantages with respect to the well-known QAM. The first advantage is its lower error probability performance, which results from better usage of the constellation space with longer minimum distances. The 2 other advantages are a lower peak to average power ratio (PAPR) and higher noise immunity. Both mathematical analysis and simulation results demonstrate that by applying standard channels in 2 cases, i.e. channels with AWGN and channels with burst noise and also with intersymbol interference (ISI) impairment simultaneously, the proposed constellation exhibits superior performance compared to the well-known QAM. As a result, this constellation is a good choice for high-speed and real-time OFDM multicarrier applications such as WiFi, WiMAX, DVB, and DAB at no extra cost.

**Key words:** Constellation, cyclic prefix, OFDM, QAM, PAPR

### 1. Introduction

Nowadays, multicarrier transmission is very popular because of the high data rate requirement of wireless systems. Orthogonal frequency-division multiplexing (OFDM) is a special case of multicarrier transmission. It is considered an effective technique for frequency-selective channels because of its spectral efficiency, its robustness in different multipath propagation environments, and its ability of combating intersymbol interference (ISI) [1]. Quadrature amplitude modulation (QAM) is an attractive technique that has been successfully implemented in multicarrier systems as well as in next generation wireless access [2,3]. The commonly used rectangular QAM constellation is, in general, suboptimal in the sense that it does not maximally space the constellation points for a given power [4]. The effectiveness of a signal constellation in digital communication systems provides a fundamental basis for the efficiency of application networks. In recent years, different constellations were designed for different modulation schemes. A concise review of the literature is considered as below. In [3], a new signal-space partitioning method is proposed for the calculation of transition probabilities of arbitrary 2-dimensional signaling with polygonal decision regions. They have shown the exact formulation of bit error probability and symbol error probability in the constellation. An algorithmic technique is presented for signal constellation design for an  $N$ -dimensional Euclidean signal space in [5]. Such signals are used for reliable and efficient digital communications on an AWGN channel. The minimum Euclidean distance between signals and

\*Correspondence: ghazimaghrebi@jdnasir.ac.ir

the constellation-constrained capacity are used as performance criteria. The authors in [6] proposed a new constellation whose shape was close to that of a snail. They compared the bit error rate (BER) performance of a 16-point non-QAM and the snail mapping with the QAM constellation. In [7], an asymptotic (large signal-to-noise ratio) expression of the minimum distance type is derived for the error rate of signal constellation in the presence of AWGN noise. The authors in [8] investigated 29 empirically generated amplitude phase keying (APK) constellation sets with  $M$ -ary alphabet sizes from 4 to 128 to determine optimum designs. The authors in [9] have considered the design of multidimensional compact constellations for minimizing the average symbol energy for a given minimum Euclidian distance between constellation points. In [10], different constellations with different mapping have been compared based on symbol error probability in the presence of strong phase noise. In [11], nonuniformly spaced (geometrically shaped) constellations are designed to maximize either joint capacity or parallel decoding capacity. The authors in [12] demonstrated different constellations and their comparison results. They proposed different parameters and based on the offered parameters, they compared different constellations. It must be noted that most of these constellations were applied for single carrier modulations. This means that considering the performance of different constellations in multicarrier modulation (MCM) mapping still is a new subject for authors.

In the literature, some authors also proposed and applied typical triangular mapping. In [13], a triangular constellation is proposed and the authors have presented the mathematical model for symbol error probability of triangular quadrature amplitude modulation in a single-input multioutput environment. The authors in [14] proposed a new code for different constellations. They have used some triangular constellations with different mapping. In [15], different constellation mappings are applied for different modulations and they are compared from different points of view. Some triangular constellations mapping are drawn. Some of the most important of these triangular constellations are demonstrated in Figure 1. Although the triangular constellation is almost a well-known mapping, as mentioned in [13–15], there are different configuration points with different specifications.

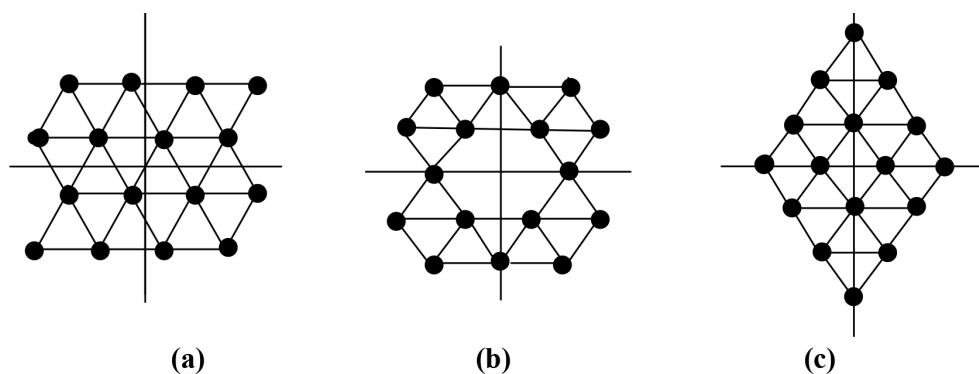


**Figure 1.** Different triangular constellations.

This paper aims to achieve more efficiently multicarrier OFDM modulation performance, only by changing its constellation configuration. For this purpose, we propose a new constellation whose points, as shown in Figure 2, are configured as a part of an equilateral triangular structure. The points of this kind of triangular constellation are symmetric with respect to the origin. However, in this configuration there are some 19 points and for achieving a good bit mapping performance 3 of these points must be omitted. In order to change this constellation to a 16-point constellation, there are different configurations, but the points of the proposed

constellation, as shown in Figure 3a, are arranged such that its error probability is less than that of the well-known QAM. It was stated in [4] that the error probability of a digital modulation depends on the reverse of the minimum distance. Based on this fact, the proposed scheme has lower BER than the QAM. In other words, the minimum distance of the propose scheme is greater than the minimum distance of the rectangular QAM constellation.

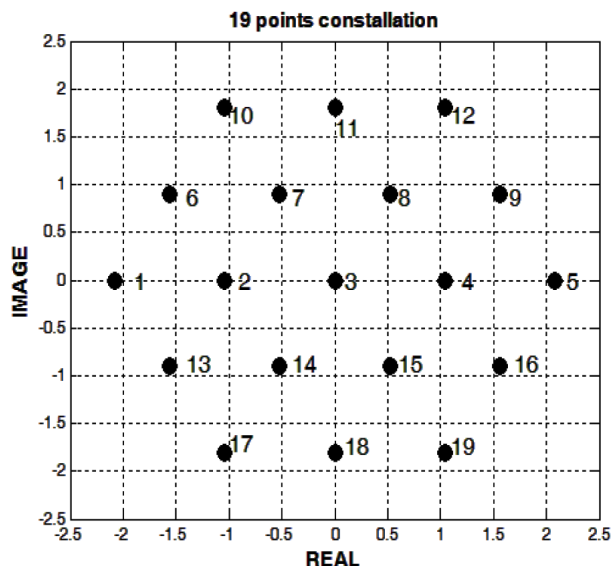


**Figure 2.** Points configuration of the 19-point triangular constellation.

Moreover, different rectangular QAMs are used in different multicarrier modulations. In the US, 64-QAM and 256-QAM are the mandated modulation schemes for digital cable as standardized by the SCTE in standard ANSI/SCTE 07 2000. In the UK, the 16-QAM and 64-QAM are standardized by the Digital Video Broadcasting-Terrestrial (DVB-T) standard [16]. In this paper, based on the DVB-T standard, a 16-point constellation is chosen.

In [17–19] the effects of cyclic prefix (CP) length in different channels for MCM are considered. CP and zero-padding are well-known prefix construction methods, the former being the most employed technique in practice due to its lower complexity [17,18]. In most digital communication systems such as practical OFDM systems, the ISI occurs due to bandlimited channels or multipath propagation. A cost-effective way for decreasing the ISI in digital communication systems such as multicarrier systems comes at the expense of the bandwidth efficiency reduction caused by inserting the CP, with the length longer than the length of the channel impulse response, to each symbol [19]. It is apparent that, for more efficiency, an OFDM modulation that can perform well at short CP lengths is highly desired [2,6].

For better and more proper comparison purposes, for bit rate efficiency point of view, Gray bit mapping is applied for the QAM and the new proposed 16-point constellation. The modulation performance may be measured in terms of the bit error rate (BER), the convergence rate, and the residual ISI. In this paper, the performance is measured by the BER criterion.

Furthermore, for better verification of the proposed scheme benefits, Stanford University Interim (SUI) standard channels with AWGN and burst noises are applied to the OFDM modulation. In each case, the channels have ISI impairment simultaneously. The mathematical analysis and simulations results show that the new constellation with the same power has a lower BER, especially for high SNRs, than the rectangular QAM.

The 6 SUI channels, as shown in Table 1, have 3 terrains: A, B, and C. These terrains have different Doppler range variation, delay spread, nonlinear of sight (NLOS), and LOS condition according to Erceg’s model [20–22]. This model is gathered by AT&T service based on extended experimental data. In this model, areas are classified in 3 terrains. Terrain A is hill areas with dense trees and high path loss. Terrain B is hills with low dense trees or a flat area with dense trees. Terrain C is flat areas with less dense trees and low path loss with respect to terrain A. In Table 2, the SUI-1 channel, for example, with its features for channel taps with different delays, is shown. Gain reduction factor (GRF) compares average power reduction for a 30 degree antenna with respect to an Omni antenna. If there is a 30 degree antenna, the determined GRF factor must be added to the path loss [20].

**Table 1.** Types of SUI channel models.

Channel	Terrain type	Doppler spread	Spread	LOS
SUI-1	C	Low	Low	High
SUI-2	C	Low	Low	High
SUI-3	B	Low	Low	Low
SUI-4	B	High	Moderate	Low
SUI-5	A	Low	High	Low
SUI-6	A	High	High	Low

**Table 2.** SUI-1 channel model.

	Tap1	Tap2	Tap3	Units
Delay	0	0.4	0.9	$\mu s$
Power (omni ant.)	0	-15	-20	dB
90% K-factor (omni)	4	0	0	
75% K-factor (omni)	20	0	0	
Power (30° ant.)	0	-21	-32	dB
90% K-factor (30°)	16	0	0	
75% K-factor (30°)	72	0	0	
Doppler	0.4	0.3	0.5	Hz

The paper is organized as follows. Mathematical analysis of ISI impairment in the OFDM system is performed in Section 2. The analysis of the OFDM modulation is described in Section 3 and mathematical analysis of the TRI constellation performance is described in Section 4. In Sections 5 and 6, simulation results and conclusions are presented, respectively.

## 2. Mathematical analysis of ISI impairment

In this section, conditions that cause ISI impairment are considered. For this propose, it is assumed that an OFDM symbol in the baseband is defined as

$$x_l[n] = \sum_{i=-N/2}^{N/2-1} a_{i,l} e^{j \frac{2\pi}{N} i n} s[n], \tag{1}$$

where  $a_{i,l}$  denotes the complex symbol modulating of the  $i$ th subcarrier,  $s[n]$  is the time window function defined in the interval  $[0, M]$ , where  $M$  is the OFDM symbol period, and  $N$  is the number of subcarriers that

are spaced  $\Delta f = 1/N$  apart. The OFDM symbol of Eq. (1) satisfies the condition of mutual orthogonality between subcarriers in the symbol interval.

In this work, it is assumed that the channel impulse response to be presented is

$$h(t) = \sum_{l=0}^L h_l \delta(t - \frac{lT}{N}) \quad (2)$$

where  $h_l$  is the mutually uncorrelated zero-mean complex Gaussian tap weight coefficients and  $T$  is the OFDM symbol period. It is assumed that the ISI on a symbol is only limited by the previous symbol.

The mathematical representation of the  $m$ th symbol of the output of the OFDM transmitter can be written as

$$x(t) = \sum_m \sum_{i=-N/2}^{N/2-1} a_{i,m} e^{j \frac{2\pi i}{T} (t-mT)} s(t-mT) \quad (3)$$

The received baseband signal at the input of the OFDM receiver will be as

$$\begin{aligned} r(t) &= h(t) * x(t) = \sum_{l=0}^L h_l x(t - \frac{lT}{N}) \\ &= \sum_{l=0}^L h_l \sum_m \sum_{i=-N/2}^{N/2-1} a_{i,m} e^{j \frac{2\pi i}{T} (t - \frac{lT}{N} - mT)} s(t - \frac{lT}{N} - mT) \end{aligned} \quad (4)$$

At the receiver side, in order to demodulate the  $k$ 'th subcarrier of the  $m$ 'th OFDM symbol and by replacing  $n$  with  $n + m'N$ , we have

$$\begin{aligned} r_{k',m'} &= \frac{1}{N} \sum_{l=0}^L h_l \sum_m \sum_{i=-N/2}^{N/2-1} a_{i,m} e^{-j \frac{2\pi i l}{N}} \\ &\quad \times \sum_{n=0}^{N-1} e^{j \frac{2\pi}{N} ((i-k')n + (m'-m)(i-k')N)} \cdot \\ &\quad \times s(\frac{nT}{N} - \frac{lT}{N} + (m'-m)T) \end{aligned} \quad (5)$$

Eq. (5) will be considered in the three following cases and since in the case of  $m \neq m'$ ,  $s[n]$  is out of the DFT region,  $0 \leq n \leq N-1$ ; therefore the result will be zero.

**Case 1.**  $m = m'$  and  $i = k'$

In this case, the  $s[n]$  region is  $l \leq n \leq N + l_g - 1$ , and then  $s[n]$  will be

$$s(\frac{nT}{N} - \frac{lT}{N} + (m'-m)T) = s(\frac{nT}{N} - \frac{lT}{N}).$$

By considering the DFT region in Eq. (5) and the  $s[n]$  region, we will have

$$r_{k',m'} = \sum_{l=0}^L h_l e^{-j \frac{2\pi l k'}{N}} (1 - \frac{l}{N}) a_{k',m'}. \quad (6)$$

**Case 2.**  $m = m'$  and  $i \neq k'$

In this case, the  $s[n]$  region is similar to the previous case and then

$$r_{k',m'} = \frac{1}{N} \sum_{\substack{i=-N/2 \\ i \neq k'}}^{N/2-1} a_{i,m'} \sum_{l=0}^L h_l e^{-j \frac{2\pi l i}{N}} \sum_{n=l}^{N-1} e^{-j \frac{2\pi}{N} (i-k')n}. \quad (7)$$

**Case 3.**  $m = m' - 1$

In this case, the  $s[n]$  region is  $l - N \leq n \leq l - 1$ , and therefore

$$s\left(\frac{nT}{N} - \frac{lT}{N} + (m' - m)T\right) = s\left(\frac{nT}{N} - \frac{lT}{N} + T\right).$$

Because it is assumed that the maximum latency  $LT/N$  is less than  $T$ , then  $N$  will be greater than  $L$  ( $L$  is the maximum length of  $l$ ). This means that the lower bound of the  $n$  region in the  $s[n]$  function will be negative. Therefore, Eq. (5) will be

$$r_{k',m'} = \frac{1}{N} \sum_{i=-N/2}^{N/2-1} a_{i,m'-1} \sum_{l=0}^L h_l e^{-j \frac{2\pi l i}{N}} \times \sum_{n=0}^{l-1} e^{-j \frac{2\pi}{N} (i-k')(n+N)}. \quad (8)$$

Finally,  $r_{k',m'}$  is the summation of Eq. (6) to Eq. (8); therefore the OFDM symbol will be

$$\begin{aligned} r_{k',m'} &= \sum_{l=0}^L h_l e^{-j \frac{2\pi k' l}{N}} \left(1 - \frac{l}{N}\right) a_{k',m'} \\ &+ \frac{1}{N} \sum_{\substack{i=-N/2 \\ i \neq k'}}^{N/2-1} a_{i,m'} \sum_{l=0}^L h_l e^{-j \frac{2\pi l i}{N}} \sum_{n=l}^{N-1} e^{-j \frac{2\pi}{N} (i-k')n} \\ &+ \frac{1}{N} \sum_{i=-N/2}^{N/2-1} a_{i,m'-1} \sum_{l=0}^L h_l e^{-j \frac{2\pi l i}{N}} \sum_{n=0}^{l-1} e^{-j \frac{2\pi}{N} (i-k')(n+N)} \end{aligned} \quad (9)$$

In Eq. (9), the first term is the desired data, scaled by a complex number depending on the channel taps. The second term represents the intercarrier interference (ICI) caused by other subcarriers belonging to the current OFDM symbol. Finally, the third term represents the ISI caused by the subcarriers of the previous OFDM symbol [23].

The ISI can be avoided by the insertion of a GI at the beginning of each OFDM symbol. The GI should be longer than the maximum possible delay spread of the channel. The GI part of each symbol is filled with copying the end part of the same symbol. In [23] it is shown that after removing GI in the receiver, the final  $r_{k',m'}$  term will be

$$r_{k',m'} = \sum_{l=0}^L h_l e^{-j \frac{2\pi k' l}{N}} a_{k',m'}, \quad (10)$$

which contains only the desired symbol, free from the ICI and ISI. Therefore, by inserting a GI longer than the maximum delay spread of the channel and by cyclically extending the OFDM symbol over the GI, one can eliminate both the ICI and ISI completely and the channel appears to be flat fading for each subcarrier.

**3. Analysis of the OFDM modulation**

OFDM is a digital MCM technique that transmits a number of narrowband slowly modulated signals instead of one wideband fast modulated signal. In traditional OFDM, a fast Fourier transform (FFT) is used to assign parallel data to orthogonal subchannels [24]. This method has some advantages such as:

1. Parallel transmission occurs over different frequencies in order to support digital data transmission in multipath fading channels, since this spreads the fading effect on many bits and degrades its effects.
2. Due to orthogonality between subchannels, their spectrums are allowed to overlap with each other, resulting in bandwidth efficiency increasing [25,26].
3. Parallel transmission also increases symbol length, leading to more robustness of the system against ISI, multipath fading channels, and wideband channels with impulse noise characteristics [25,27].
4. Because of using the FFT, traditional OFDM is a comparable low complexity MCM technique [26,28].

With the aid of the IFFT and appending a CP between the individual blocks at the transmitter and taking the FFT at the receiver, a broadband frequency-selective channel is converted into a set of parallel flat fading subchannels or tones [29].

In this paper, for more efficiency, it is assumed that the channel impulse response,  $\mathbf{h} = [h_0, \dots, h_L]$ , is longer than the CP length and therefore the system suffers from ISI. In this case, the transmitted symbol at time  $k - 1$  will contribute to the received symbol at time  $k$  as the below matrix equation [30]. In this case, it is assumed that  $X_i^{(k)}$  and  $Y_i^{(k)}$ ,  $i = 1, 2, \dots, N$  are the FFTs of the  $i$ th element of the transmitted and received symbols at time  $k$ , respectively, and also  $\mathbf{I}$  and  $\mathbf{0}$  are the ‘identity’ and ‘zero’ matrices, respectively. Therefore,  $\mathbf{I}_v$  and  $\mathbf{I}_N$  are identity matrices with  $v \times v$  and  $N \times N$  sizes, respectively.  $\mathbf{F}_N$  is the  $N \times N$  DFT matrix.

$$\begin{aligned}
 - \begin{bmatrix} Y_1^{(k)} \\ \vdots \\ Y_N^{(k)} \end{bmatrix} &= \mathbf{F}_N \begin{bmatrix} \left| \begin{array}{cccc} h_L & \cdots & h_{v+1} \\ 0 & \ddots & \vdots \\ \vdots & 0 & h_L \\ 0 & \cdots & 0 \end{array} \right. \\ 0 \end{bmatrix} \cdot P \cdot \begin{bmatrix} x_1^{(k1)} \\ \vdots \\ x_N^{(k1)} \end{bmatrix} \\
 + \mathbf{F}_N \begin{bmatrix} h_v & \cdots & \cdots & h_0 & 0 & \cdots & \cdots & \cdots & 0 \\ h_{v+1} & h_v & \cdots & \cdots & h_0 & 0 & \cdots & \cdots & \vdots \\ [1ex] \vdots & \ddots & \ddots & \ddots & \ddots & \ddots & \ddots & \ddots & \vdots \\ h_L & \cdots & \ddots & \ddots & \ddots & \ddots & h_0 & 0 & \vdots \\ 0 & h_L & \cdots & \ddots & \ddots & \ddots & \ddots & h_0 & 0 \\ 0 & 0 & h_L & \cdots & \cdots & \cdots & \cdots & \cdots & h_0 \end{bmatrix} \cdot P \cdot \begin{bmatrix} x_1^{(k)} \\ \vdots \\ x_N^{(k)} \end{bmatrix} \tag{11}
 \end{aligned}$$

with

$$P = \begin{bmatrix} \mathbf{0} | I_v \\ I_N \end{bmatrix},$$

where  $v$  is the length of CP. Now suppose that  $\mathbf{F}_N$  is an  $N \times N$  IDFT matrix; then the demodulated received symbol in Eq. (11) becomes

$$-\mathbf{Y} = \mathbf{F}_N T^{(k1)} P \cdot \mathbf{F}_N \cdot \mathbf{X} + \mathbf{F}_N T^{(k)} P \cdot \mathbf{F}_N \cdot \mathbf{X} - \tag{12}$$

The 2 terms  $\mathbf{T}^{(k)} \mathbf{P}$  and  $\mathbf{T}^{(k-1)} \mathbf{P}$  on the right-hand side of Eq. (12) are not circulant. Therefore, for the case  $L + 1 > v$ , the ISI is not removed and the undesired contributions in  $Y_i^{(k)}$  from subsymbols that differ from  $X_i^{(k)}$  are the interferences [30].

#### 4. Mathematical analysis of the TRI constellation performance

The average power ( $P_{QAM}$ ) and the error probability ( $P_{e(QAM)}$ ) for the rectangular 16-QAM, as shown in Figure 3b, with a minimum distance of  $2d$  and a noise variance of  $\sigma^2$ , and also the Gray bit mapping are defined in terms of the Q-function as below [15]

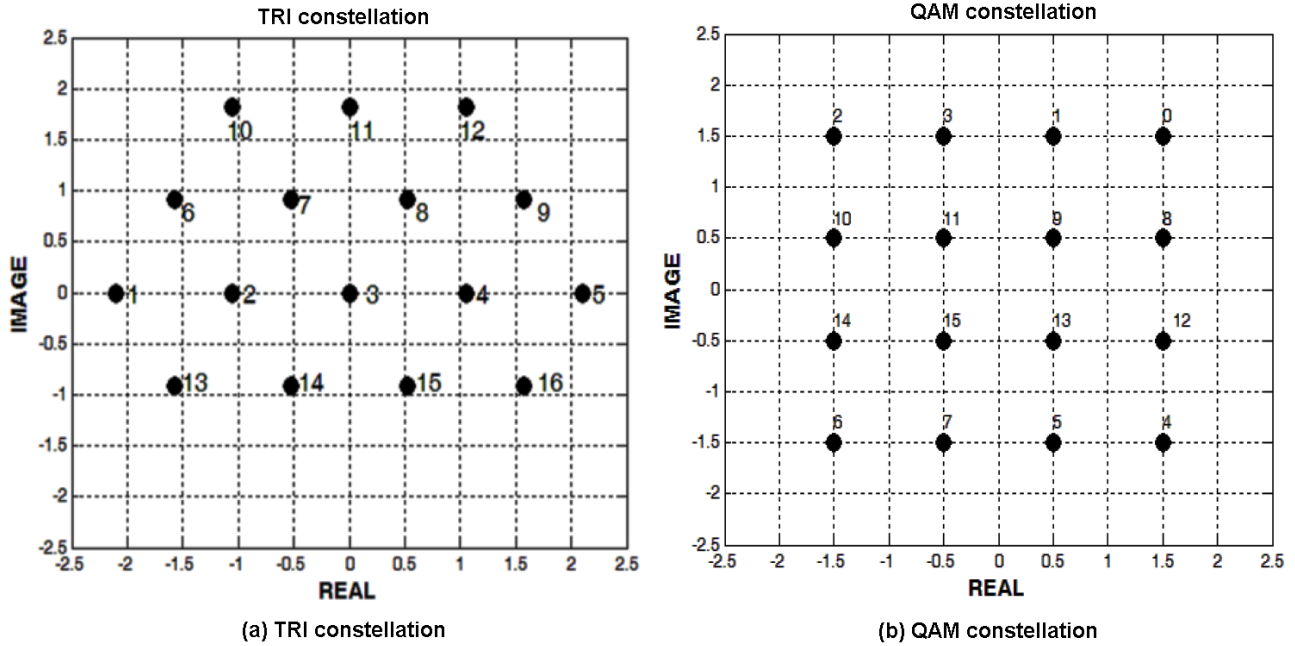


Figure 3. QAM and TRI constellations.

$$P_{e(QAM)} = 3Q\left(\frac{d}{\sigma}\right) \quad P_{QAM} = 10d^2 \tag{13}$$

The new proposed constellation is a part of the triangular constellation, which is shown in Figure 3a. The points of this constellation are positioned on the vertex points of equilateral triangular structures. Therefore, we named it triangular form (TRI). In the TRI constellation, it is assumed that  $2d_1$  is the minimum distance between 2 adjacent points and  $\sigma^2$  is the noise variance. Therefore, the constellation average power by averaging the summation of all power points will be

$$P_{TRI} = 9.25d_1^2. \tag{14}$$



For comparison, it is assumed that the QAM and the TRI constellations have the same average power. For this propose,  $d_1$  will be

$$9.25d_1^2 = 10d^2 \Rightarrow d_1 = 1.039d. \tag{15}$$

It is obvious that the minimum distance of the TRI is longer than that of the rectangular QAM, and as a result it has a lower error probability with respect to the QAM. For computing the error probability of the TRI constellation, we numbered, as in Figure 3a, the constellations points. The TRI constellation points, for error probability computations, based on the number of adjacent points for each point (and as a result, the same error probability), are divided into 5 groups as below.

- a) The 6 points of Figure 3a, labeled as {1, 5, 10, 12, 13, 16} , have 3 adjacent points. Therefore, the error probability of these 6 points is 3 times the error probability of each point as below

$$P_{e1} = 6 \times 3Q \left( \frac{d_1}{\sigma} \right) = 18Q \left( \frac{d_1}{\sigma} \right) \tag{16}$$

- b) The 5 vertices points, labeled as {6, 9, 11, 14, 15} , have 4 adjacent points. Therefore, their error probability will be

$$P_{e2} = 5 \times 4Q \left( \frac{d_1}{\sigma} \right) = 20Q \left( \frac{d_1}{\sigma} \right) \tag{17}$$

- c) The 5 vertices points labeled as {2, 3, 4, 7, 8} are adjacent to 6 other adjacent points. Therefore, the error probability of these points will be

$$P_{e3} = 5 \times 6Q \left( \frac{d_1}{\sigma} \right) = 30Q \left( \frac{d_1}{\sigma} \right) \tag{18}$$

It must be noted, considering the Q-function properties, in computing the error probability of each point, as the error probability of the QAM modulation, only the nearest points are taken into account and the points with longer distances are ignored. Moreover, it is assumed that the points are transmitted with the same probability. Therefore, the total error probability of the TRI constellation, with substitution  $d_1 = 1.039d$ , is the average of Eq. (6) through Eq. (8) as below

$$P_{e(TRI)} = \frac{P_{e1} + P_{e2} + P_{e3}}{16} = 4.25Q \left( \frac{d_1}{\sigma} \right) = 4.25Q \left( 1.039 \frac{d}{\sigma} \right). \tag{19}$$

Comparing Eq. (13) and Eq. (19) and considering the Q-function table, it is obvious that the error probability of the TRI constellation, especially for high values of  $d_1/\sigma$  or high SNR, is less than that of the rectangular QAM. Therefore, the mathematical analysis shows that the new proposed constellation has an error probability lower than that of the QAM.

The 2 other specifications for constellations comparison are the peak to average power ratio ( $PAPR$ ) and the noise immunity  $\eta$ , which are defined respectively as below [12]

$$PAR = 10 \log_{10} \left( \frac{\max_k(P_k)}{P} \right) + 3 \quad (dB) \tag{20}$$

$$\eta = 20 \log_{10} \frac{\min_{i,j}(d(i,j))}{\sqrt{P}d_2} \quad (dB) , \quad (21)$$

where  $P_k$  is the power of the  $k$ th point,  $P$  is the average power of the constellation,  $d_2$  is the minimum distance of a 2-QAM, and  $d(i, j)$  is the distance between the 2 points  $i$  and  $j$ . The *PAPR* defines the linear operation area of the system. Signals with a higher *PAPR* require higher precision components [12]. This parameter for these constellations is computed as below

$$PAR_{QAM} = 10 \log_{10} \left( \frac{4.5}{2.5} \right) + 3 = 5.55 \quad (dB) \quad (22)$$

$$PAR_{TRI} = 10 \log_{10} \left( \frac{(2.079)^2}{2.5} \right) + 3 = 5.37 \quad (dB) \quad (23)$$

It is obvious that the second advantage of the TRI constellation is its lower *PAPR* with respect to that of the QAM. It is clear that the lower the *PAPR*, the better the constellation.

The noise immunity,  $\eta$ , defines the difference in SNR, necessary to ensure the same average error probability [12]. The third advantage of the new constellation is its  $\eta$  higher than that of the QAM, which are computed as below

$$\eta_{QAM} = 20 \log_{10} \frac{1}{\sqrt{2.5}} = -3.98 \quad (dB) \quad (24)$$

$$\eta_{TRI} = 20 \log_{10} \frac{1.039}{\sqrt{2.5}} = -3.53 \quad (dB) \quad (25)$$

Finally, for more verification of the advantages of the TRI constellation, the minimum distances of the 3 triangular constellations in Figure 1 are computed as below. The constellation of Figure 1a, as proposed in [13], has 8 couple points with the same distance to the origin. It means that the points in each couple have the same error probability. Now suppose that  $2x_1$  is the minimum distance between 2 adjacent points and  $\sigma^2$  is the noise variance. Therefore, the constellation average power by averaging the summation of all power points will be

$$P_1 = \left( \frac{144}{16} \right) x_1^2. \quad (26)$$

For comparison, it is assumed that the QAM and this constellation have the same average power. For this propose,  $x_1$  will be

$$\left( \frac{144}{16} \right) x_1^2 = 10d^2 \Rightarrow x_1 = 1.035d. \quad (27)$$

Referring to Eq. (15), this constellation is better than the QAM, but the TRI constellation is better than this constellation.

Now suppose that in the constellation of Figure 1b, as proposed in [15],  $2x_2$  is the minimum distance between 2 adjacent points and  $\sigma^2$  is the noise variance. In this case, there are 4 groups of 4 points with the same distance to the origin. Therefore, the constellation average power will be

$$P_2 = \left( \frac{192}{16} \right) x_2^2. \quad (28)$$

Assume, for comparison, the QAM and this constellation have the same average power. For this purpose,  $x_2$  will be

$$\left( \frac{192}{16} \right) x_2^2 = 10d^2 \Rightarrow x_2 = 0.94d \quad (29)$$

This means that the minimum distance of this constellation is smaller than that of the QAM and as a result the performance of QAM and TRI is better than that of this constellation.

The constellation of Figure 1c, as proposed in [15], has 4 groups of couple points and 2 groups of 4 points with the same distance to the origin. Suppose that  $2x_3$  is the minimum distance between 2 adjacent points and  $\sigma^2$  is the noise variance. Thus, the constellation average power of all power points will be

$$P_3 = \left(\frac{160}{16}\right)x_3^2. \tag{30}$$

For comparison, it is assumed that the QAM and this constellation have the same average power. For this purpose,  $x_3$  will be

$$\left(\frac{160}{16}\right)x_3^2 = 10d^2 \Rightarrow x_3 = d. \tag{31}$$

The performance of this constellation is the same as that of QAM and is lower than that of the TRI constellation. These computations show that the minimum distances of these 3 triangular constellations are not greater than those of the TRI constellation, and as a result it is obvious that the proposed TRI constellation has better performance, i.e. lower BER, than these 3 constellations.

**5. Simulation results**

In this work, the OFDM transceiver of Figure 4 was simulated. The random serial input data are modulated through a constellation mapper and then converted to a discrete time blocks through 256-IFFT. In this system, SUI-1 through SUI-6 standard channels with 3 taps and AWGN and burst noises are used. For transmission efficiency, the CP length was set 1 symbol, i.e. the CP length is smaller than the channel impulse response length with 3 taps. This means that the implemented system will suffer from ISI. At the receiver, we convert the channel output from serial to parallel and after removing CP from each symbol, FFT is taken, and then we extract the main symbol. A novel 16-point triangular constellation (TRI) and 16-QAM, with Gray bit mapping and their specifications, as shown in Table 3, are applied to the OFDM transceiver. In this simulation, it is assumed the minimum distance of QAM constellation is  $d = 1$  and therefore the minimum distance of the TRI constellation will be 1.039. For comparison, it is assumed these two constellations have the same average power with the amount of  $P = 2.5$ .

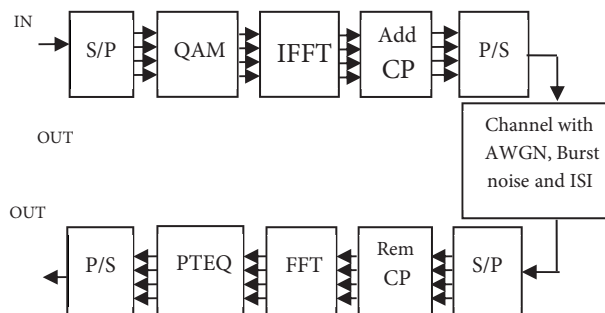


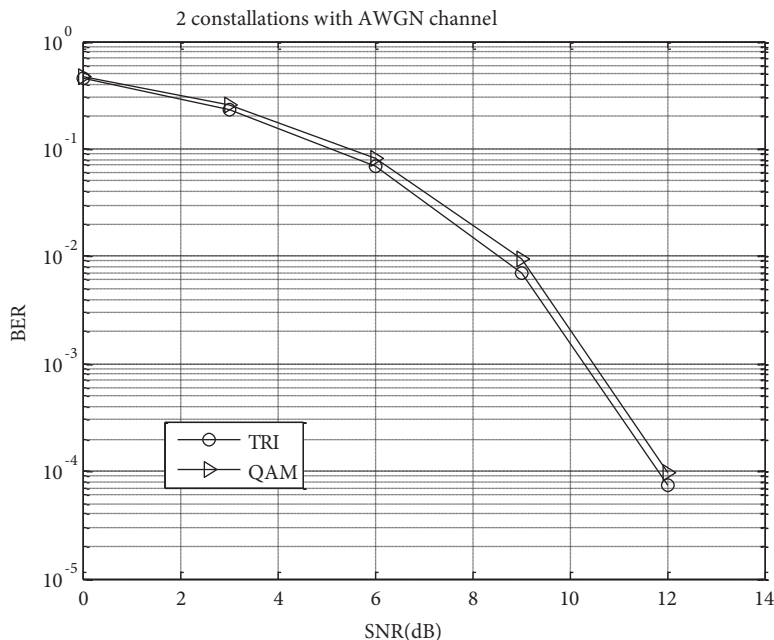
**Figure 4.** The OFDM transceiver block diagram.

For verifying the TRI constellation, 3 experiments by MATLAB software have been performed on the OFDM transceiver. In each experiment, 100,000 data blocks have been sent and the program has been run 1000

**Table 3.** Main parameters of constellations.

Parameter	$P$	$PAR$ [dB]	$d$	$H$ [dB]
QAM	2.5	5.55	1	-3.98
TRI	2.5	5.37	1.039	-3.53

times for each channel realization and the average values of the simulation runs have been calculated. In the first experiment the applied channel is AWGN with zero mean and standard deviation 1. The results of this experiment are shown in Figure 5. It is obvious the TRI constellation has better performance, in BER, than the QAM constellation. In the second experiment, 6 standard channels, SUI[1] through SUI[6], and an AWGN noise (with zero mean) were employed and in the third experiment, burst noise was employed. Burst noise is a kind of noise that occurs suddenly and affects stochastically a part of the data stream. The parameters of the burst noise, i.e. duration, power, and position of its occurrence, were produced with normal standard distribution  $N(0,1)$ , i.e. normal distribution with zero mean and unit variance. This means that we have stochastically changing based on  $N(0,1)$  distribution for the duration, power, and position of occurrence of the noise in the channel for each realization. For each experiment, the BER is the criterion obtained from the ensemble average of 1000 independent Monte Carlo simulation repetitions.

**Figure 5.** Performance of TRI and QAM constellations with AWGN channel.

Because the results are almost the same, for the second and third experiments, only the results for SUI[1] channel are shown in Figures 6 and 7. Simulation results show that the TRI constellation has a lower error probability, especially for high SNRs, than the well-known rectangular QAM in the both channels. It must be noted that in our simulations co-channel interference caused by the other transmitter's OFDM signals are not considered.

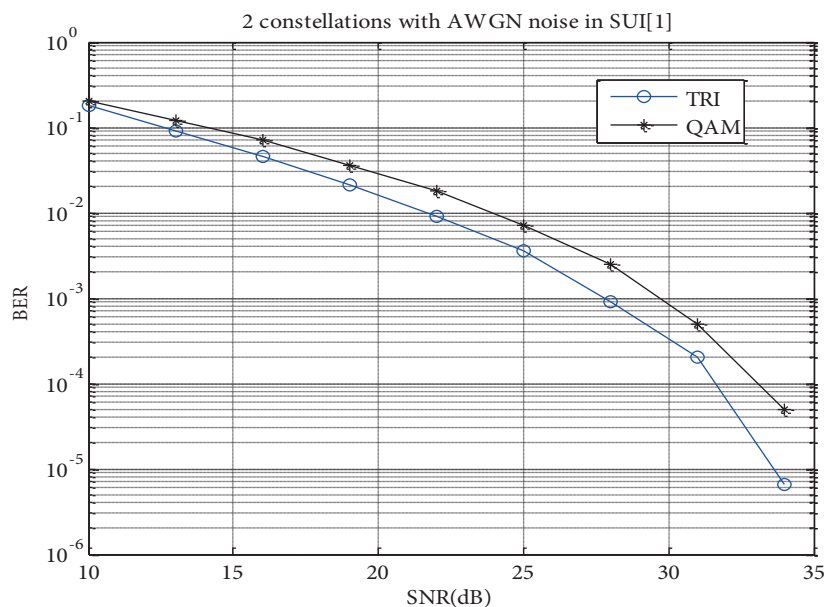


Figure 6. Performance of TRI and QAM constellations with AWGN noise with ISI.

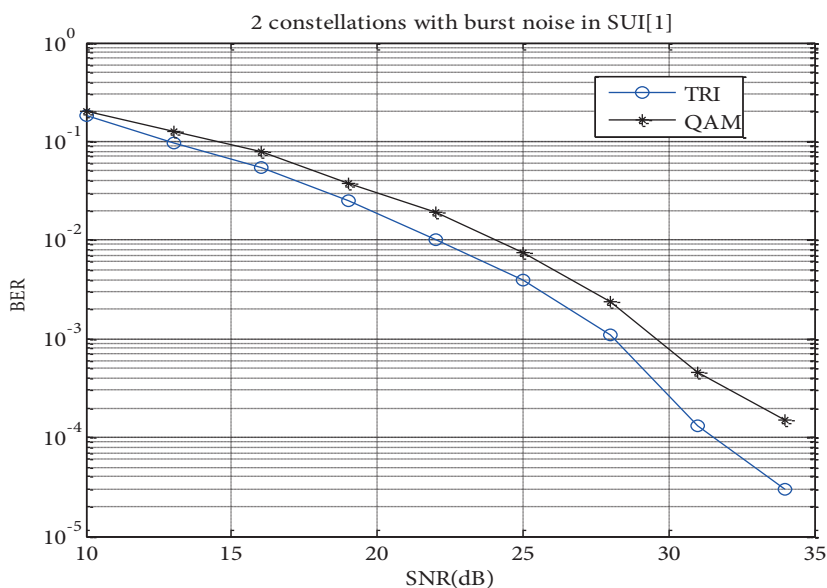


Figure 7. Performance of the TRI and QAM constellations in the presence of AWGN and burst noise with ISI.

### 6. Conclusion

In this work, a special triangular TRI constellation was introduced for OFDM applications. The performance of this constellation was measured against the well-known QAM constellation for SUI channels with the AWGN and burst noises and also with ISI impairment simultaneously. The simulation results verify that the TRI constellation, with an insufficient length of CP, has lower BER and PAPR, while it has higher  $\eta$  than the QAM. Therefore, the proposed constellation is a suitable candidate to replace the rectangular QAM in multicarrier modulations such as OFDM.

## References

- [1] Yalçın M, Akan A, Doğan H. Low-complexity channel estimation for OFDM systems in high-mobility fading channels. *Turk J Elec Eng & Comp Sci* 2012; 20: 583-592.
- [2] Rugini L, Banelli P. BER of OFDM systems impaired by carrier frequency offset in multipath fading channels. *IEEE T Wirel Commun* 2005; 4: 2279-2288.
- [3] Xiao L, Dong X. The exact transition probability and bit error probability of two-dimensional signaling. *IEEE T Wirel Commun* 2005; 4: 2600-2609.
- [4] Proakis J, Salehi M. *Digital communications*. 5th edition, New York, NY, USA: McGraw-Hill, 2007.
- [5] Porath JE, Aulin T. Design of multidimensional signal constellations. *IEE P-Commun* 2003; 150: 317-323.
- [6] Ghazi-Maghrebi S, Ghanbari M, Lotfizad M. Two novel constellation algorithms for discrete multi-tone. *Electron Lett* 2009; 45: 1260-1261.
- [7] Foschini G, Gitlin R, Weinstein S. Optimization of two-dimensional signal constellations in the presence of Gaussian noise. *IEEE T Commun* 1974; 22: 23-38.
- [8] Thomas CM, Weidner MY, Durrani SH. Digital amplitude-phase keying with M-ary alphabets. *IEEE T Commun* 1974; 22: 168-180.
- [9] Beko M, Dinis R. Designing good multi-dimensional constellations. *IEEE Wireless Commun Lett* 2012; 1: 221-224.
- [10] Krishnan R, Amat A, Eriksson T, Colavolpe G. Constellation optimization in the presence of strong phase noise. *IEEE T Commun* 2013; 61: 5056-5066.
- [11] Barsoum MF, Jones C, Fitz M. Constellation design via capacity maximization. *IEEE International Symposium on Information Theory* 2007; 1821-1825.
- [12] Golden P, Jacobsen K, Dedieu H. *Fundamentals of DSL Technology*. Boca Raton, FL, USA: Auerbach Publications, 2006.
- [13] Haider Qureshi F, Amin Sheikh S, Umar Khan Q, Mumtaz Malik F. SEP performance of triangular QAM with MRC spatial diversity over fading channels, Qureshi et al. *EURASIP Journal on Wireless Communications and Networking* 2016; 5: DOI 10.1186/s13638-015-0511-2.
- [14] Su W, Xia XG. Signal constellations for quasi-orthogonal space-time block codes with full diversity. *IEEE T Inf Theory* 2004; 50: 2331-2347.
- [15] Xiong F. *Digital Modulation Techniques*. First ed. Boston, MA, USA: Artech House, 2000.
- [16] Purkayastha BB, Sarma KK. *A Digital Phase Locked Loop based Signal and Symbol Recovery System for Wireless Channel*. New Dehli, India: Springer, 2015.
- [17] Yildiz H, Acar Y, Cooklev T, Dogan H. A generalised prefix for space-time block-coded orthogonal frequency division multiplexing wireless systems over correlated multiple-input multiple output channels. *IET Commun* 2014; 8: 1589-1598.
- [18] Cooklev T, Dogan H, Cintra RJ, Yildiz, H. A generalized prefix construction for OFDM systems over quasi-static channels. *IEEE T Veh Technol* 2011; 60: 3684-3693.
- [19] Fazel K, Kaiser S. *Multi-Carrier and Spread Spectrum Systems*. Chichester, UK: John Wiley & Sons, 2003.
- [20] Jain R. Channel models: A Tutorial. *WiMAX Forum*, Feb. 2007.
- [21] Erceg V, Hari KVS, Smith MS, Baum DS, Sheikh KP, Tappenden C, Costa JM, Bushue C, Sarajedini A, Schwartz R et al. Channels models for fixed wireless applications. *IEEE 802.163c-01-29r4*, July 2001.
- [22] Erceg V, Greenstein LJ, Tjandra Y, Parkoff SR, Gupta A, Kulic B, Julius AA, Bianchi R. An empirically based on path loss model for wireless channels in suburban environments. *IEEE J Sel Area Comm* 1999; 17: 1205-1211.
- [23] Ghazi-maghrebi S, Motahayeri H, Der Avanesian K, Lotfizad M. A New Mathematical Analysis of the Cyclic Prefix Effect On Removing ISI and ICI in DMT Systems, *IEEE International conference TENCON2011*, Nov. 2011; 1-4.

- [24] Ghaith A, Hatoum R, Mrad H, Alaeddine A. Performance analysis of the wavelet-OFDM new scheme in AWGN channel. *IEEE Communications and Information Technology* 2013; 225-229.
- [25] Narayan M, Mohanty, Mishra S. Design of MCM based Wireless System using Wavelet Packet Network & its PAPR Analysis. *IEEE, International Conference on Circuits, Power and Computing Technologies* 3013; 821-824.
- [26] Asif R, Hussaini A, Abd-Alhameed R, Jones S, Noras J, Elkhazmi E, Rodriguez J. Performance of different wavelet Families using DWT and DWPT-channel equalization using ZF and MMSE. *8th IEEE Design and Test Symposium* 2013; 1-6.
- [27] Banerjee S, Jeyakumar A, Nar V. Wavelet packet modulation for mobile communication. *IJERA* 2013; 3:1016-1022.
- [28] Negash BG, Nikookar H. Wavelet-based multicarrier transmission over multipath wireless channels. *Electron Lett* 2000; 36: 1787-1788.
- [29] Kim JW, Lee YH. Modified frequency-domain equalization for channel shortening in reduced-CP OFDMA systems. *IEEE T Commun* 2007; 55: 1825-1836.
- [30] Acker KV, Moonen M, Pollet T. Per-tone equalization for DMT-based systems. *IEEE T Commun* 2001; 49: 109-119.